Science and Technology of Welding and Joining

ISSN: (Print) (Online) Journal homepage: https://www.tandfonline.com/loi/ystw20

Dissimilar friction stir welding of pure Ti and carbon fibre reinforced plastic

Jeong-Won Choi , Yoshiaki Morisada , Huihong Liu , Kohsaku Ushioda , Hidetoshi Fujii , Kimiaki Nagatsuka & Kazuhiro Nakata

To cite this article: Jeong-Won Choi , Yoshiaki Morisada , Huihong Liu , Kohsaku Ushioda , Hidetoshi Fujii , Kimiaki Nagatsuka & Kazuhiro Nakata (2020): Dissimilar friction stir welding of pure Ti and carbon fibre reinforced plastic, Science and Technology of Welding and Joining, DOI: 10.1080/13621718.2020.1788814

To link to this article: https://doi.org/10.1080/13621718.2020.1788814

Published online: 08 Jul 2020.

SCIENCE AND TECHNOLOGY OF WELDING AND JOINING
https://doi.org/10.1080/13621718.2020.1788814

The Institute of Materials, Minerals and Mining

Taylor & Francis
Taylor & Francis Group

Dissimilar friction stir welding of pure Ti and carbon fibre reinforced plastic

Jeong-Won Choi, Yoshiaki Morisada, Huihong Liu, Kohsaku Ushioda, Hidetoshi Fujii, Kimiaki Nagatsuka and Kazuhiro Nakata

Joining and Welding Research Institute, Osaka University, Osaka, Japan

ABSTRACT

Dissimilar friction stir welding was conducted on the combination of pure Ti and carbon fibre reinforced plastic. The weld interface microstructure and mechanical properties of the obtained joints were systematically investigated. Before welding, a surface treatment was performed on the Ti surface using a silane coupling agent. As a result, the silane coupling agent treatment helped to fabricate the sound dissimilar Ti/CFRP joint. The dissimilar Ti/CFRP joints obtained at the interface temperature between the melting point of the CFRP and thermal decomposition point of the CFRP showed superior tensile-shear strength due to the formation of the sufficient reaction between the surface-modified Ti and CFRP and the suppression of welding defect formation in the CFRP near the weld interface.

ARTICLE HISTORY
Received 31 March 2020
Revised 18 June 2020
Accepted 21 June 2020

KEYWORDS
Microstructure; mechanical properties; friction stir welding (FSW); dissimilar; Ti; carbon fibre reinforced plastic (CFRP)

Introduction

In recent years, extensive efforts have been made regarding the dissimilar welding of metals and CFRP because the dissimilar joints of metals and CFRP are expected to incorporate the advantage of each material, such as high ductility and compressive strength of metals and significant weight reduction due to CFRP. However, it is quite challenging since the metals and CFRP show completely different physical and electrochemical properties [1].

In previous studies, laser welding [2,3], ultrasonic welding [4,5], friction spot welding [6,7] and riveted hybrid welding [8] were used in order to fabricate the sound dissimilar joints of metals and CFRP. Jung et al. welded stainless steel to CFRP using the laser direct joining process and reported that the obtained dissimilar joints were not sound and mainly fractured at the weld interface and the melted zone of the CFRP [2,3]. The limitations of laser welding include an insufficient pressure during the lap joining process which leads to the formation of defects such as voids at the weld interface. The sound dissimilar joints of metals and CFRP can be fabricated by ultrasonic welding and friction spot welding techniques because the interface temperature can be easily controlled and the formation of defects such as voids at the weld interface can be suppressed by the deformation due to the applied pressure from the tool [4–7]. However, the dimensions of the dissimilar joints are limited. In the case of rivet welding, rivets cannot typically be used depending on the shape and location of the joint and the effective cross-sectional area is reduced because the joint materials need to be drilled.

Friction stir welding (FSW), as a solid-state welding technique invented by The Welding Institute (TWI), can solve the dimensional problem and simultaneously suppress the welding defects formation by the applied pressure from the tool and the easy control of the interface temperature. Sound dissimilar Al/CFRP [9] and Fe/CFRP [10] joints were fabricated by FSW. Nagatsuka et al., one of the present authors, successfully obtained the sound dissimilar joints of the A5052 alloy and CFRP, and reported that a MgO oxide layer formed at the weld interface allowed the dissimilar Al alloy and CFRP to be joined without welding defects formation at a critical welding speed [9]. Additionally, Nagatsuka et al. fabricated the dissimilar joints of SPCC (conventional low carbon steel)/Polyamide 6 and SPCC/Polyethylene using FSW [10], because both polyamide 6 and polyethylene are typically used as thermoplastic resins. The authors investigated the effect of the pre-welding surface treatment of the polyethylene and reported that the dissimilar SPCC and polyamide 6 could be directly welded, while the SPCC and polyethylene could not be directly joined using FSW. A corona discharge treatment of the polyethylene surface facilitated the direct joining between the dissimilar polyethylene and SPCC by FSW [10]. However, the dissimilar joints fabricated by the corona discharge surface treatment of the polyethylene surface still showed insufficiently strong interfaces that make them fracture at the weld interfaces. Even

CONTACT Hidetoshi Fujii fujii@jwri.osaka-u.ac.jp Joining and Welding Research Institute, Osaka University, Osaka, Ibaraki 567-0047, Japan

though the dissimilar joints of Al/CFRP and Fe/CFRP were previously fabricated using FSW as already mentioned, they showed a high risk of galvanic corrosion, in which the corrosion may occur in the metallic materials having a relatively low electric potential when they were joined to an electrochemically noble material such as CFRP [11]. Ti, which is a much nobler metallic material compared with Al and Fe, shows a great potential to significantly reduce the galvanic corrosion risk in the dissimilar joint of Ti and CFRP. Although the combination of the dissimilar Ti/CFRP, which is electrochemically more promising, using riveted hybrid joining technique was previously investigated [8], no investigation of the dissimilar Ti/CFRP FSW has been reported. In the present study, pure Ti and CFRP were adopted to investigate the feasibility for obtaining the sound Ti–CFRP joints during FSW. The FSW parameter of the tool rotation speed was optimised in order to achieve a sound dissimilar joint of Ti and CFRP with high bonding strength. The optimum interface temperature for the dissimilar FSW of Ti and CFRP was investigated for the first time by examining the weld interface microstructure and mechanical properties of the obtained Ti/CFRP joints.

Experimental procedure

The pure Ti plate with the dimensions of 150 mm^L × 50 mm^W × 2 mm^T and CFRP plate (polyamide 6

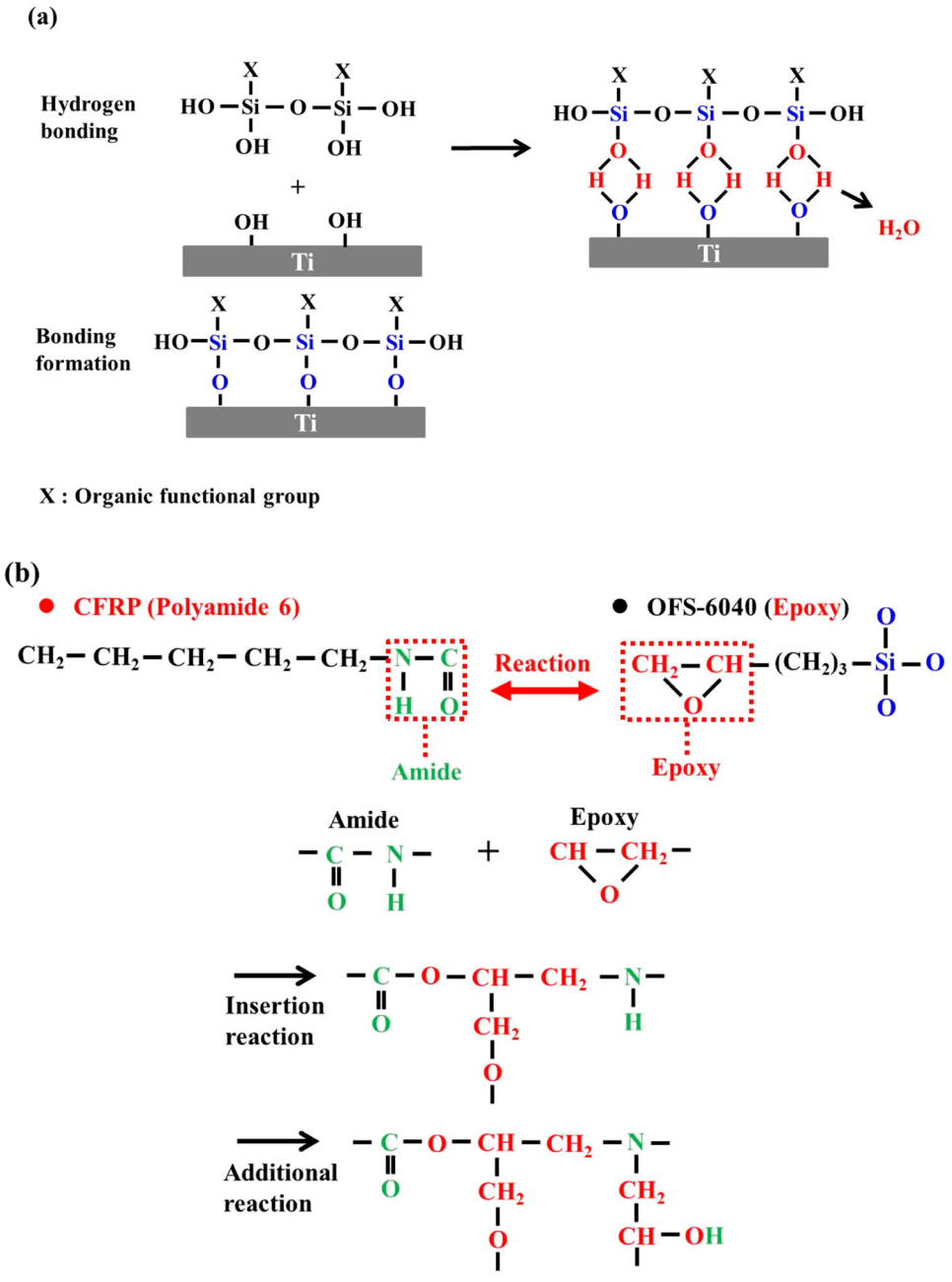

Figure 1. (a) The bonding mechanism between the silane coupling agent and Ti surface and (b) the detailed illustrations of the chemical structures of CFRP and silane coupling agent (OFS-6040), and the chemical reaction between the amide group and epoxy group.

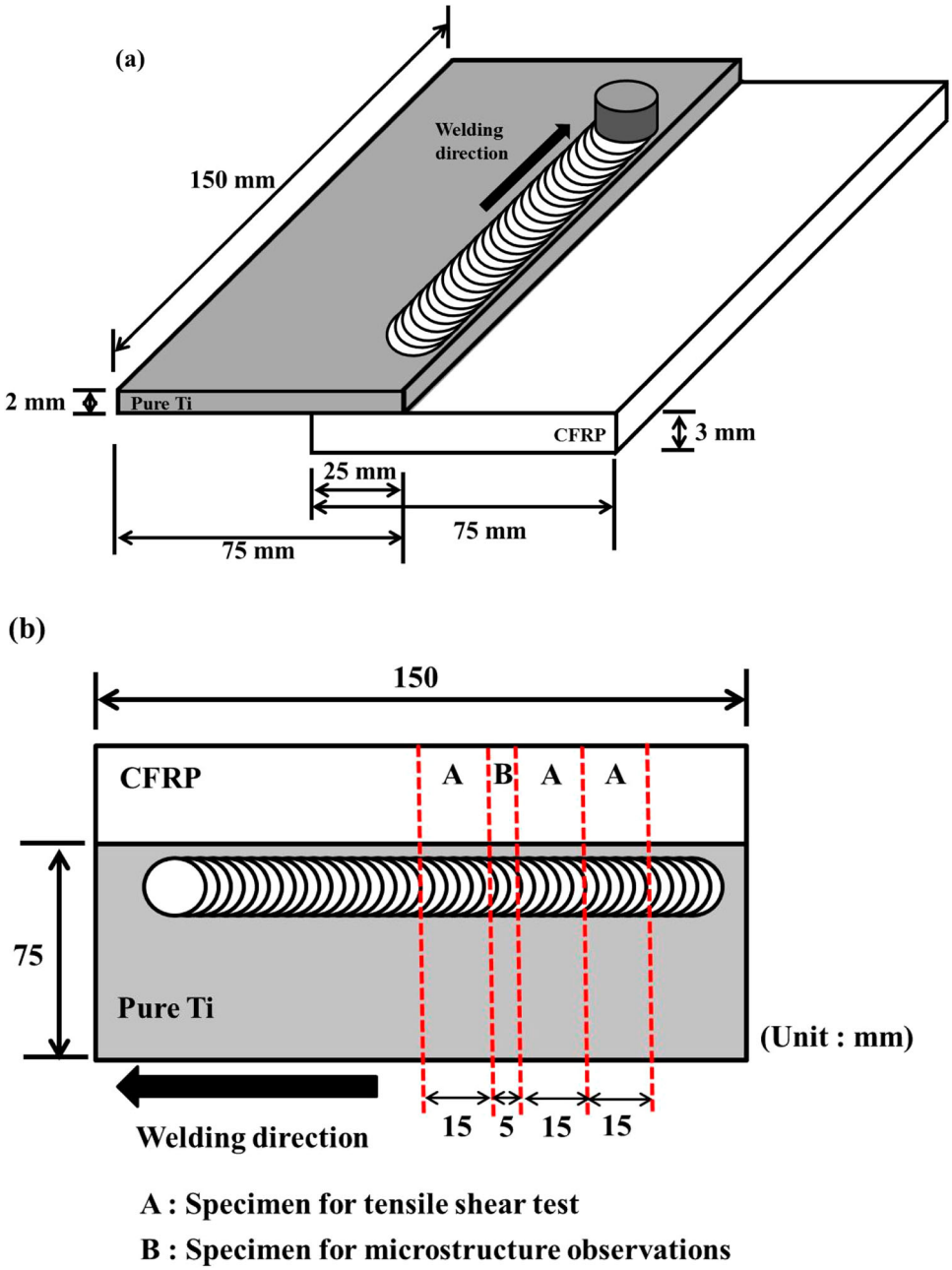

Figure 2. (a) The detailed descriptions of the FSW process and (b) the specimen preparations.

with 20 wt-% carbon fibre addition) with the dimensions of 150 mm^L × 50 mm^W × 3 mm^T were used as the weld materials. The surface treatment using an OFS-6040 silane coupling agent (3-Glycidoxypropyl trimethoxysilane, Epoxy functional group) was carried out on the pure Ti surface since polyamide 6 has the amide group, which can react with the epoxy group [12]. Figure 1(a) shows the widely known bonding mechanism between the silane coupling agent and the Ti surface. When the silane coupling agent and the distilled water are mixed, the reactive silanol (Si–OH) species are generated by hydrolysis. These reactive silanol groups show a high congeniality with each other, which leads to the formation of the –Si–O–Si– bond with some parts of the hydroxyl groups by a condensation reaction. The silane coupling agent experienced by the hydrolysis and condensation reactions physically absorbs the hydroxyl groups of the Ti by hydrogen bonding. When heating is subsequently performed, the hydrogen bond between the silanol and the hydroxyl group of Ti is converted into the covalent –Si–O–Ti– bond [13]. Then, the Ti surface with an organic functional group can be obtained. However, the reaction between the polymer and the silane coupling agent cannot occur unless the reactivity of the polymer matches that of the silane coupling agent, i.e. not all the organic functional groups contained in the silane coupling agent are suitable for bonding to the polymer [12]. Since polyamide 6 has the amide group, which can react with the epoxy group, the silane coupling agent, OFS-6040 (3-Glycidoxypropyl trimethoxysilane, Epoxy functional group), which contains an epoxy group, was

Table 1. The detailed welding parameters used in this study.

	Welding parameters
Tool rotation speed (rev min^{-1})	50, 100, 125, 150, 175, 200, 250, 300
Concentrations of silane coupling (%)	3.5
Plunge depth (mm)	0.9
Welding speed (mm min^{-1})	100
Tilting angle (°)	3
Shielding gas	Ar

used in this study. Figure 1(b) shows the detailed illustrations of the chemical structures of CFRP and silane coupling agent (OFS-6040), and the chemical reaction between the amide group and epoxy group. During the reaction between the amide and epoxy groups, the insertion reaction of the epoxy group first occurs between the C molecule and N molecule of the amide group, followed by the additional reaction of the epoxy group to the imino group generated by splitting of the amide bond.

The surfaces of the pure Ti and CFRP plates were mechanically polished in advance with abrasive papers up to 3000 and 240 grit, respectively. The pure Ti plates were then immersed in an aqueous solution of the OFS-6040 silane coupling agent mixed with distilled water at the silane coupling agent concentration of 3.5%, followed by drying under a vacuum atmosphere at 120°C for 1 h.

During FSW, the pure Ti plate was placed on the top, and the CFRP plate was placed on the bottom side. The detailed description of FSW is schematically illustrated in Figure 2(a). FSW was carried out at various tool rotation speeds varying from 50 to 300 rev min^{-1} at a constant welding speed of 100 mm min^{-1} and plunge depth of 0.9 mm. Ar gas was injected to prevent oxidation during FSW. A tungsten carbide (WC)-based tool with a shoulder diameter of 15 mm without a probe was used in the present study and the tool tilt angle was 3°. The specific welding parameters are listed in Table 1. The interface temperature profiles for the dissimilar Ti/CFRP FSW conducted at the various tool rotation speeds were measured by a K-type thermocouple inserted into the centre of the weld interface between the pure Ti and CFRP.

Tensile-shear specimens with a length of 125 mm and a width of 15 mm were prepared by a container machine from the obtained joints with the tensile axis perpendicular to the welding direction as illustrated in Figure 2(b). The specimens were then subjected to the tensile-shear test at a constant crosshead speed of 0.5 mm min^{-1}. A measurement of the tensile-shear strength of the dissimilar lap joint was implemented by pulling at both ends until the joint fails in shear, then it is reported as the tensile force divided by the shear area. The transverse cross-section specimens of the obtained joints were prepared by the container machine as illustrated in Figure 2(b), and mechanically polished with abrasive papers up to 4000 grit followed by a final mirror-polish with 1 μm diamond suspensions. The specimens were then subjected to the microstructure analysis by an optical microscope (OM) and a scanning electron microscope (SEM).

Results and discussion

Effect of tool rotation speed on mechanical properties of the joint

FSW was conducted at various tool rotation speeds ranging from 50 to 300 rev min^{-1} with a constant silane coupling agent concentration of 3.5% and plunge depth of 0.9 mm in order to investigate the effect of the frictional heat input on the dissimilar joints of Ti and CFRP. Figure 3 shows the results of the tensile-shear strength and the peak interface temperature of the joints as a function of tool rotation speed and the corresponding fracture positions. The tensile-shear strength increases with the increasing tool rotation speed from 50 to 125 rev min^{-1}. It then saturates between 125 and 175 rev min^{-1}, followed by the significant decrease in the tensile-shear strength with the further increase in the tool rotation speed from 200 to 300 rev min^{-1}. The joints fabricated at the rotation speeds of 50 and 100 rev min^{-1} fractured at the weld interface. Meanwhile, the joints fabricated at the rotation speeds of 125, 150 and 175 rev min^{-1} fractured in the CFRP base material outside of the stir zone as shown in Figure 3(b). The joints fabricated at the rotation speeds of 200, 250 and 300 rev min^{-1} fractured inside the stir zone on the CFRP side, which was attributed to the softening of the CFRP due to the high frictional heat generated during FSW. The temperature dependence of the CFRP tensile strength was reported in previous studies [14,15]. The strength of the CFRP matrix is known to strongly depend on the working temperature (i.e. thermal history) and it usually decreases with the increasing working temperature. In addition, the peak interface temperature experienced in the dissimilar Ti/CFRP joints fabricated at the different tool rotation speeds are also indicated in Figure 3(a). The results indicate that the peak interface temperature increases with the increasing tool rotation speed from 50 to 300 rev min^{-1} due to the increased frictional heat input generated during FSW. It is worthy to note that the joints fabricated at the tool rotation speeds of 125, 150 and 175 rev min^{-1}, which exhibited the highest tensile-shear strength, had the peak interface temperature within the range between the melting temperature (225°C) and the decomposition temperature (350°C) of the CFRP. Above the decomposition temperature of the CFRP, the tensile-shear strength of the joints significantly decreased with the increasing interface temperature. This result is attributed to the CFRP decomposition above 350°C, which is in agreement with the

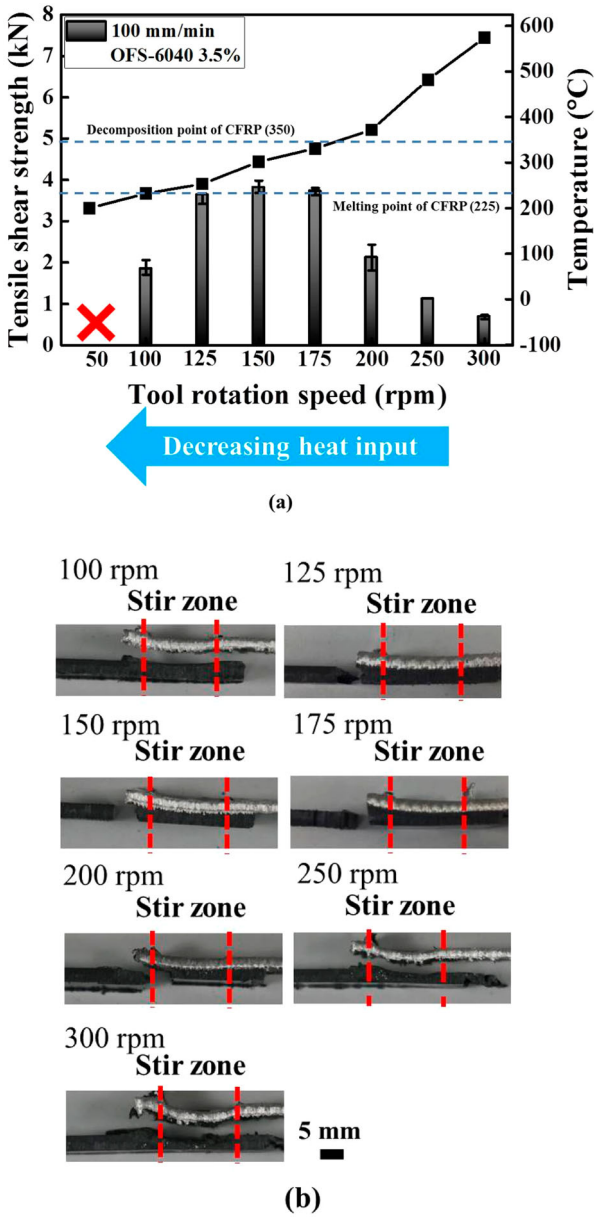

Figure 3. (a) The tensile-shear strength and interface temperature of the dissimilar Ti/CFRP joints fabricated at different tool rotation speeds and (b) the corresponding fracture sites.

previous studies [14,15]. On the other hand, the joint fabricated at the tool rotation speed of 100 rev min^{-1}, which had the peak interface temperature close to the melting point of the CFRP, showed a clearly decreased tensile-shear strength. For the joint fabricated at the much lower tool rotation speed of 50 rev min^{-1}, whose peak interface temperature was about 200°C and lower than the CFRP melting point, the pure Ti and CFRP were completely unbonded. This result implies that the silane coupling agent applied on the pure Ti surface cannot react with the CFRP when the interface temperature is lower than the melting point of the CFRP. This is because the FSW process is completed in a short time, thus it is difficult for the molecules of the CFRP and the silane coupling agent to bond with each other when the CFRP and the silane coupling agent are in the solid state.

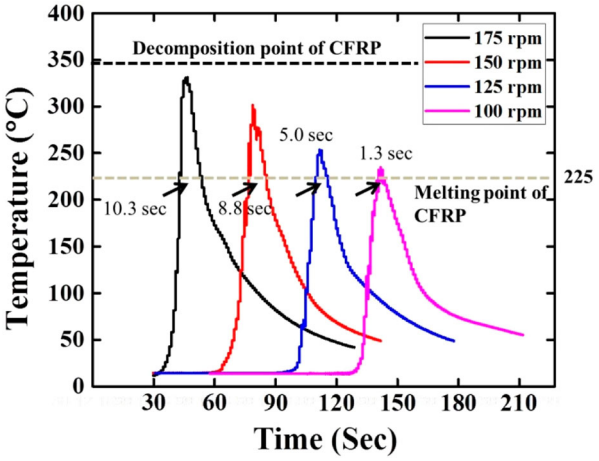

Figure 4. The interface welding temperature histories experienced in the dissimilar Ti/CFRP joints fabricated at different tool rotation speeds.

The temperature histories experienced in the dissimilar joint fabricated between the melting point and the thermal decomposition point of CFRP are shown in Figure 4. The joints fabricated at the tool rotation speed of 125 ~ 175 rev min^{-1}, which had the highest tensile-shear strength, underwent the molten states of the CFRP for 5.0, 8.8 and 10.3 s, respectively. However, that fabricated at the tool rotation speed of 100 rev min^{-1}, which had a lower tensile-shear strength, only underwent the molten state for only 1.3 s. Based on the obtained results, it can be inferred that both the sufficient interface temperature and sufficient maintenance in the molten state of the CFRP are required to obtain the sound dissimilar joint of Ti and CFRP even though the dissimilar joint can be successfully bonded when the peak interface temperature is above the melting point of the CFRP. Based on a previous study on the reaction of organic materials with a silane coupling agent [15], the above results are considered to be attributed to the following hypothesis based on the viewpoint of diffusion of the CFRP and silane coupling agent molecules. In the case of the joint fabricated at the tool rotation speed of 100 rev min^{-1}, the reaction regions between the silane coupling agent on the Ti surface and CFRP were insufficient, thus making the weld interface weak and fractured, while in the case of joints fabricated at the tool rotation speed of 125 ~ 175 rev min^{-1}, the dissimilar joint had a sufficiently strong weld interface due to the sufficient formation of the reaction regions between the silane coupling agent and CFRP, thereby leading to the fracture inside the CFRP.

Effect of welding temperature on interfacial microstructure of the joint

The transverse cross-sections of the joints fabricated at the various tool rotation speeds were subjected to

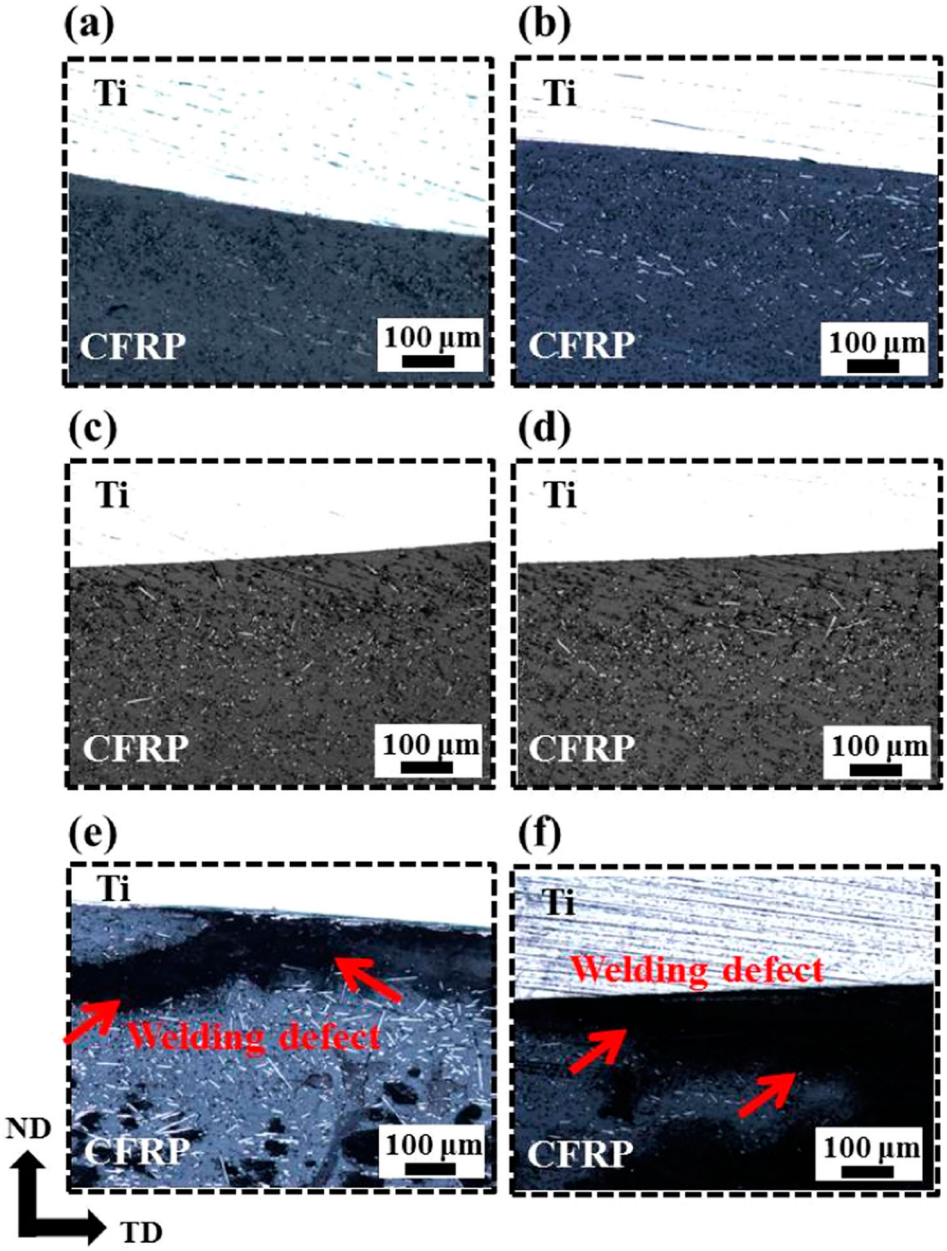

Figure 5. OM observations of the CFRP near the weld interfaces on the cross sections of the joints fabricated at the tool rotation speeds of (a) 100 rev min^{-1}, (b) 125 rev min^{-1}, (c) 150 rev min^{-1}, (d) 175 rev min^{-1}, (e) 200 rev min^{-1} and (f) 300 rev min^{-1}.

OM observations; the results are shown in Figure 5. In the joints fabricated at the tool rotation speeds ranging from 100 to 175 rev min^{-1}, no welding defects formed near the weld interface. However, in the joints fabricated at the tool rotation speeds of 200 and 300 rev min^{-1}, the welding defects formed at the CFRP matrix near the weld interfaces, and the amount and thickness of the welding defects increased with increasing the tool rotation speed. The formation mechanism of the welding defects in the CFRP during the dissimilar welding of the metal and CFRP has been previously reported [16]. When the interface temperature is higher than the thermal decomposition temperature of the CFRP (350°C), the CFRP pyrolysis occurs. During pyrolysis, the crosslink reaction occurs, which leads to the dehydration. The pyrolysis of the amide bond subsequently occurs, which generates a large amount of gases such as CO_2, NH_3, H_2O and hydrocarbons, leading to the formation of defects [16]. The formation of the welding defect is in accordance with the previous results reported by Xu et al. [17]. These results imply that the formation of welding defects in the CFRP near the weld interface depends on the frictional heat input. In other words, they form when the interface temperature exceeds the thermal decomposition temperature of the CFRP and the amount of the welding defects increases with the increasing interface temperature. Therefore, the fracture was prone to occur at this position which reduced the tensile-shear strength of the joint. In the joint obtained at the tool rotation speed of 300 rev min^{-1}, the occurrence of pyrolysis was promoted at a higher welding temperature. Thus,

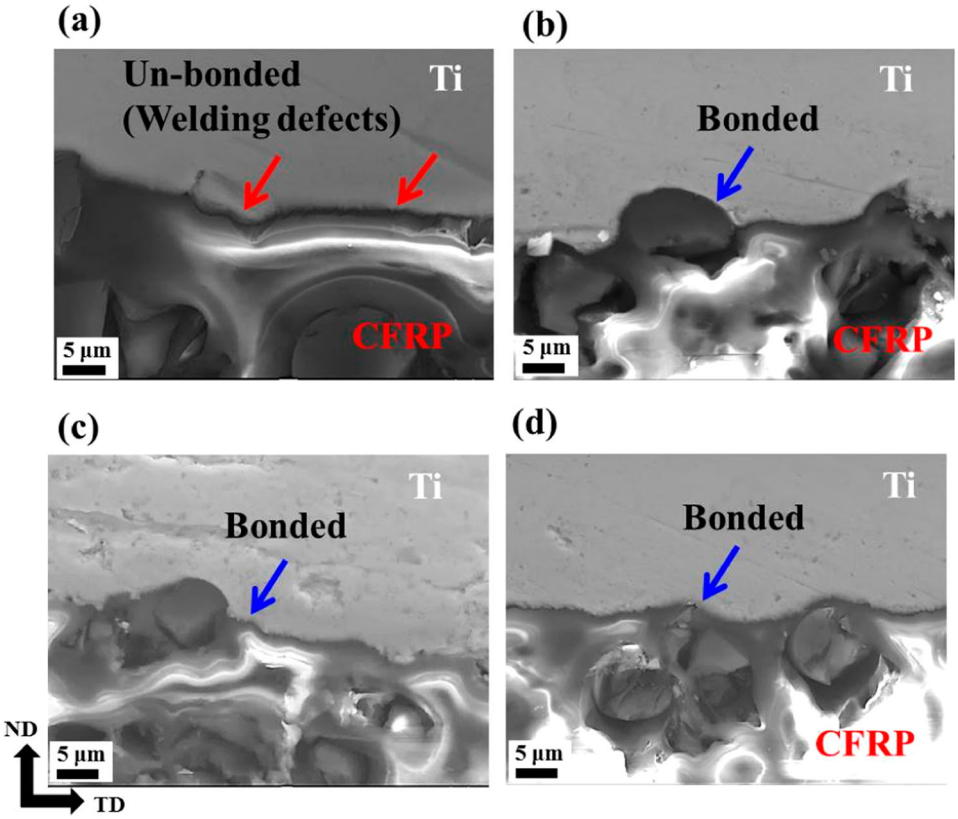

Figure 6. SEM microstructure of the cross sections of the dissimilar Ti/CFRP joints fabricated at different tool rotation speeds of (a) 100 rev min^{-1}, (b) 125 rev min^{-1}, (c) 150 rev min^{-1} and (d) 175 rev min^{-1}.

crystallisation rarely occurred and the thicker welding defects formed, which further decreased the tensile-shear strength of the joint.

In order to further examine the weld interfaces of the joints, the cross-section specimens of the dissimilar Ti/CFRP joints fabricated at different tool rotation speeds were subjected to SEM observations, and the results are shown in Figure 6. The presence of the welding defects as indicated by the red arrows can be observed at the weld interface at the tool rotation speed of 100 rev min^{-1}. This result is considered to be attributed to a short duration in the molten state of the CFRP, which leads to an insufficient reaction between the silane coupling agent applied on the Ti surface and the silane coupling agent [15]. Therefore, it induces the occurrence of the unbonded region between the CFRP and the silane coupling agent, inducing the welding defect at the weld interface as shown in 6a. The dissimilar Ti/CFRP joints obtained at the tool rotation speeds varying from 125 to 175 rev min^{-1} show fully bonded weld interfaces with the absence of any defects, which is due to the sufficient duration in the molten state of the CFRP that allows a sufficient reaction between silane coupling agent and CFRP. On the other hand, in the joints fabricated at 200 and 300 rev min^{-1}, since a higher interface temperature than the thermal decomposition point of the CFRP was experienced in the joints fabricated at 200 and 300 rev min^{-1}, several gases such as CO_2, NH_3, H_2O and hydrocarbons were generated from the CFRP, causing the welding defects formation in the CFRP matrix near the weld interface.

Effect of welding temperature on defect formation

Two types of welding defects can be identified in the present study. The type 1 welding defects are considered to be related to the gas generations such as CO_2, NH_3, H_2O and hydrocarbons from the CFRP near the weld interface at a high welding temperature [16], while the type 2 welding defects are considered to be caused by the insufficient reaction between the silane coupling agent applied on the Ti surface and CFRP at a low welding temperature and insufficient duration [15].

Consequently, the temperature dependence of the welding defect formation can be summarised as illustrated in Figure 7. Below the melting temperature of the CFRP, it is considered that the silane coupling agent cannot react with the CFRP during FSW, so that the pure Ti and CFRP were unable to be bonded (Figure 7(a)). At the temperature higher than 350°C, the Ti/CFRP can be completely welded due to the sufficiently high frictional heat input, even though the interface temperature was higher than the thermal decomposition temperature of the CFRP. However, due to the generation of gases such as CO_2, NH_3, H_2O and hydrocarbons, only partial crystallisation occurred in the microstructure of the CFRP near the weld interface, leading to the formation of the type 1 welding

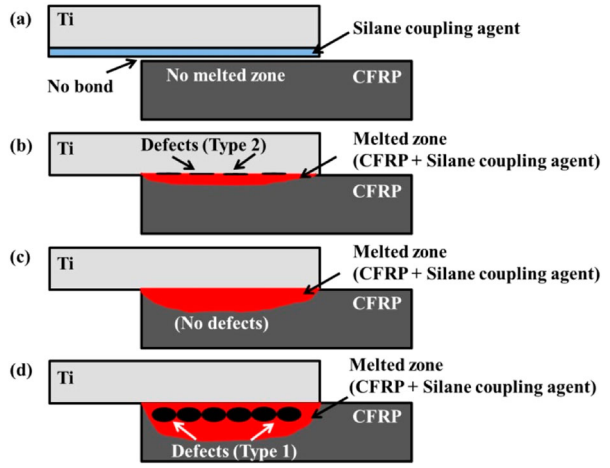

Figure 7. Schematic illustrations of the joints fabricated at different interface temperature of (a) below 225°C, (b) between 225 and 350°C (insufficient duration) (c) between 225 and 350°C (sufficient duration) and (d) above 350°C.

defects as shown in Figure 7(d). At the welding temperature between the melting point and thermal decomposition point of the CFRP at which the maximum shear strength was achieved, the joints have a completely bonded weld interface of the Ti and CFRP due to the sufficient duration in the molten state of CFRP, which induces to sufficient reaction between the silane coupling agent applied on the pure Ti surface and CFRP, and the microstructure of the CFRP near the weld interface was completely crystallised after cooling with the absence of the defects presumably due to the appropriate frictional heat input generated during FSW (Figure 7(c)). Nevertheless, if the duration in the melt state of the CFRP during FSW is too short (1.3 s), the type 2 welding defects were generated at the weld interface as shown in Figure 7(b), which was caused by the insufficient reaction between the silane coupling agent and the CFRP during FSW [15]. These welding defects made the dissimilar joints prone to fracture at the weld interface, resulting in low tensile-shear strength. Therefore, the interface temperature between the melting point and thermal decomposition point of the CFRP with the simultaneous guarantee of the sufficient duration of the CFRP melt state during FSW is considered to be optimum in terms of the highest tensile-shear strength among the examined joints and the fracture at the CFRP matrix outside of the stir zone (Figure 7(b)).

Conclusions

Dissimilar FSW was performed on pure Ti and CFRP plates. The welding parameters, focusing on the tool rotation speeds, were optimised in order to obtain a sound dissimilar Ti/CFRP joint. The findings obtained are as follows.

(1) The dissimilar Ti/CFRP joints fabricated at the welding temperature between the melting point of the CFRP and thermal decomposition point of the CFRP with a sufficient duration in the melt state of the CFRP showed the highest tensile-shear strength among the examined joints and fractured at the CFRP matrix outside of the stir zone.
(2) When the duration of the CFRP melt state is insufficient during FSW, the welding defects were generated at the weld interface of the joint, which was caused by the insufficient reaction between the silane coupling agent and the CFRP, leading to the low tensile-shear strength.
(3) Below the melting temperature of the CFRP (225°C), the pure Ti and CFRP were unable to be bonded since the silane coupling agent cannot react with the CFRP during FSW.
(4) At a temperature higher than the thermal decomposition of the CFRP (350°C), the Ti/CFRP can be completely welded due to the sufficient high frictional heat input during FSW. However, due to the generation of gases such as CO_2, NH_3, H_2O and hydrocarbons, only partial crystallisation occurred in the CFRP near the weld interface, causing the formation of welding defects in the CFRP, which weakened and fractured the dissimilar joints at the CFRP stir zone.

Acknowledgements

This study was supported by JST-Mirai Program Grant Number JPMJMI19E5, and a Grant-in-Aid for Science Research from the Japan Society for the Promotion of Science.

Disclosure statement

No potential conflict of interest was reported by the author(s).

Funding

This study was supported by JST-Mirai Program [grant number JPMJMI19E5], and a Grant-in-Aid for Science Research from the Japan Society for the Promotion of Science.

References

[1] Liu FC, Liao J, Nakata K. Joining of metal to plastic using friction lap welding. Mater Des. 2014;54:236–244.
[2] Jung KW, Kawahito Y, Katayama S. Laser direct joining of carbon fibre reinforced plastic to stainless steel. Sci Technol Weld Joining. 2011;16:676–680.
[3] Jung KW, Kawahito Y, Takahashi M, et al. Laser direct joining of carbon fiber reinforced plastic to zinc-coated steel. Mater Des. 2013;47:179–188.
[4] Konchakova N, Balle F, Barth FJ, et al. Finite element analysis of an inelastic interface in ultrasonic welded metal/fibre-reinforced polymer joints. Comput Mater Sci. 2010;50:184–190.
[5] Balle F, Wagner G, Eifler D. Ultrasonic metal welding of aluminum sheets to carbon fibre reinforced thermoplastic composites. Adv Eng Mater. 2009;11:35–39.

[6] Amancio-Filho ST, Bueno C, dos Santos JF, et al. On the feasibility of friction spot joining in magnesium/fiber-reinforced polymer composite hybrid structures. Mater Sci Eng A. 2011;528:3841–3848.
[7] Yusof F, Miyashita Y, Seo N, et al. Utilising friction spot joining for dissimilar joint between aluminium alloy (A5052) and polyethylene terephthalate. Sci Technol Weld Joining. 2011;17:544–549.
[8] Kashaev N, Ventzke V, Riekehr S, et al. Assessment of alternative joining techniques for Ti–6Al–4V/CFRP hybrid joints regarding tensile and fatigue strength. Mater Des. 2015;81:73–81.
[9] Nagatsuka K, Yoshida S, Tsuchiya A, et al. Direct joining of carbon-fiber-reinforced plastic to an aluminum alloy using friction lap joining. Compos Part B. 2015;73:82–88.
[10] Nagatsuka K, Kitagawa D, Yamaoka H, et al. Friction lap joining of thermoplastic materials to carbon steel. ISIJ Int. 2016;56:1226–1231. 181–186.
[11] Palani S, Hack T, Deconinck J, et al. Validation of predictive model for galvanic corrosion under thin electrolyte layers: an application to aluminium 2024-CFRP material combination. Corros Sci. 2014;78:89–100.
[12] Materne T. Organosilane technology in coating applications: review and perspectives, Form No. 26-1402A-01. Midland (MI): Dow Corning Corporation; 2012; p. 1–16.
[13] Xie Y, Hill CAS, Xiao Z, et al. Silane coupling agents used for natural fiber/polymer composites: a review. Compos Part A. 2010;41:806–819.
[14] Wang K, Young B, Smith ST. Mechanical properties of pultruded carbon fibre-reinforced polymer (CFRP) plates at elevated temperatures. Eng Struct. 2011;33:2154–2161.
[15] Wang YC, Wong PMH, Kodur V. An experimental study of the mechanical properties of fibre reinforced polymer (FRP) and steel reinforcing bars at elevated temperatures. Compos Struct. 2007;80:131–140.
[16] Tan X, Zhang J, Shan J, et al. Characteristics and formation mechanism of porosities in CFRP during laser joining of CFRP and steel. Compos Part B. 2015;70:35–43.
[17] Xu M, Liu B, Zhao Y, et al. Direct joining of thermoplastic ABS to aluminum alloy 6061-T6 using friction lap welding. Sci Technol Weld Joining. 2020;25:391–397.